Robust Communication in Bursty Impulsive Noise and Rayleigh Block Fading

Ahmed Mahmood[†], Mandar Chitre[†*]
[†]Acoustic Research Laborotary, National University of Singapore, Singapore 119227
[*]Dept. of Electrical and Computer Engineering, National University of Singapore, Singapore 117576
{tmsahme, mandar}@nus.edu.sg

ABSTRACT

Acoustic systems operating in warm shallow waters need to be robust against impulsive noise. The latter arises from the collective snaps of snapping shrimp populaces that naturally inhabit such waters. Besides being impulsive, the noise realizations also exhibit dependency between closely spaced samples. The implicit memory of such processes cause impulses to cluster together, which makes the process bursty. In our work, we consider the stationary α-sub-Gaussian noise with memory order m (αSGN(m)) model, which characterizes both the impulsiveness and burstiness of a noise process. The model is derived from the family of heavy-tailed symmetric α-stable (SαS) distributions. We investigate the error performance of various detectors for a passband single-carrier communication scheme in αSGN(m) with Rayleigh block fading. The maximum-likelihood (ML) detector is derived and modified robust detectors are proposed by extending the framework of generalized ML estimation theory to the αSGN(m) model. Detailed simulation results are presented to quantify the error performance of the detectors and carrier placement in αSGN(m).

1. INTRODUCTION

A digital communications system is typically optimized for a Gaussian noise process [22, 26]. However, when the noise is impulsive, a significant number of outliers is observed in the received data [11, 28]. Gaussian models fail to characterize this phenomenon, which is modeled well by *heavy-tailed* (algebraic-tailed) distributions [11]. Moreover, signal processing schemes optimized for Gaussian processes are found to be *very* sub-optimal in impulsive noise scenarios [1, 8, 12, 16]. A good communication system should thus employ techniques *robust* to outliers observed in the channel.

A number of robust measures have been proposed in the literature to mitigate impulsive noise [1, 6, 8, 12]. Most of these are based on the assumption that the noise process is *white*, i.e., the observations are independent and identically distributed (IID) random variables. One such example is the white symmetric α-stable noise (WSαSN) model, whose samples are IID heavy-tailed symmetric α-stable (SαS) random variables [6, 12]. Conventional notions of robustness find their roots within optimality arguments in white impulsive noise [1, 6, 8, 12]. Though important and intuitive in their own right, there is a gap between theory and practice: ambient noise is seldom white [11, 28]. Few studies have been devoted to understanding the dependence between the noise samples. Research on the noise process in warm shallow underwater channels, powerlines and wireless interference have shown that whiteness assumptions are far from perfect [4, 10, 11, 13, 28]. Such works have deemed the noise process to be *bursty* as well as impulsive. A consequence of this is that closely-spaced samples are highly correlated. Therefore, the notion and results of *conventional robustness* may not extend to practical scenarios.

Very recently, the statistics of multiple noise data sets in warm shallow waters were analyzed [13]. The soundscape in such scenarios is impulsive due to snaps created by the snapping shrimp. By presenting delay scatter-plots, the authors observed the joint-distribution of closely-spaced samples to exhibit heavy-tailed *near-elliptic* structures. Noting that the empirical amplitude distribution of the noise data is tracked well by the heavy-tailed symmetric SαS distribution [3, 11], the authors proposed a novel model, namely, the stationary α-sub-Gaussian noise with memory order m (αSGN(m)) model [13]. With appropriately tuned parameters, realizations of αSGN(m) imitated the statistical characteristics of empirical data sets very well [13]. The model constrains each sample to be a SαS random variable, while the dependence between adjacent samples is characterized by a multivariate α-sub-Gaussian distribution. The latter is essentially a heavy-tailed *elliptic* SαS distribution [19]. A conducive property stemming from the adopted framework is that the noise process is stationary Markov [13]. Our research is motivated by underwater acoustic noise and is based on the αSGN(m) model. Though other colored impulsive noise models do exist [4, 17], they are yet to be substantiated by practical data sets. A comparison between these models is provided in [13, 24].

The contributions of this paper are as follows: We investigate the performance of common robust methods in αSGN(m) with Rayleigh block fading for an uncoded single-carrier communication scheme. The employed detectors are based on the *generalized* maximum-likelihood (ML) framework, which assumes white noise [1, 8]. We work with the passband model as matched-filtering based down conversion is known to be suboptimal in impulsive noise [12, 15, 16].

WUWNET '16, October 24-26, 2016, Shanghai, China

DOI: http://dx.doi.org/10.1145/2999504.3001111

Due to the white assumption, the aforementioned *conventional* robust methods are sub-optimal in αSGN(m). We therefore derive the optimal detector and modify the generalized ML framework to exploit the implicit memory in the αSGN(m) model. A simulation-based analysis is conducted for both severely and slightly impulsive noise with the aforementioned *conventional* and *modified* robust detectors. Comments on carrier placement are made as well.

The remainder of this paper is organized as follows: In Section 2 we present the passband system model and the αSGN(m) process. In Section 3 we discuss the ML detector for WSαSN and *generalized* ML detection in white impulsive noise. This is followed by a derivation of the ML and modified robust detectors for αSGN(m) in Section 4. We wrap up by presenting our results and conclusions in Section 5 and Section 6, respectively.

2. CHANNEL MODEL

2.1 The Passband Channel

We now briefly introduce the mathematical setup for the problem. Let $x = x_I + jx_Q$ denote the transmitted symbol that is uniformly chosen from a constellation of size M and $h = |h|e^{j\phi}$ as the complex channel tap in a block flat-fading channel. Then given a symbol rate of T, the passband receive-transmit equation of a single-carrier communication scheme is given by

$$r(t) = \Re\left\{h\sqrt{\frac{2}{\mathcal{E}_g}}g(t)xe^{j2\pi f_c t}\right\} + w(t)$$
$$= |h|\big(x_I\ell_I(t,\phi) + x_Q\ell_Q(t,\phi)\big) + w(t), \quad (1)$$

for $t \in (0, T]$ [22]. Here f_c is the carrier frequency, $w(t)$ is the additive noise component and

$$\ell_I(t,\phi) = \sqrt{\frac{2}{\mathcal{E}_g}}g(t)\cos(2\pi f_c t + \phi) \quad \text{and}$$
$$\ell_Q(t,\phi) = -\sqrt{\frac{2}{\mathcal{E}_g}}g(t)\sin(2\pi f_c t + \phi)$$

are the (phase rotated) I and Q carriers, respectively. The baseband signal shaping pulse is given by $g(t)$ and its energy by $\mathcal{E}_g$. We assume Rayleigh fading, therefore h is a sample outcome of a zero-mean circularly symmetric complex Gaussian random variable with variance σ_h^2, i.e., $\mathcal{CN}(0, \sigma_h^2)$. By constraining f_c to be a multiple of $1/T$, $\ell_I(t,\phi)$ and $\ell_Q(t,\phi)$ are orthonormal over $t \in (0, T]$, this is implicitly assumed.

The primary reason for working with the passband model and not the conventionally adopted baseband model is that the latter implicitly assumes a linear passband-to-baseband conversion block. This is typically implemented via matched-filtering with respect to $\ell_I(t,\phi)$ and $\ell_Q(t,\phi)$ [22]. This operation is optimal if $w(t)$ is a Gaussian noise process, but performance degrades significantly if the noise is impulsive [12].

In certain channels such as underwater acoustics, system bandwidths typically run into the tens/hundreds of kilohertz [25]. Such scenarios allow employing a sampling block at the front-end of the receiver thus effectively discretizing the received passband signal. If f_s is the sampling frequency, then to satisfy the Nyquist criterion, one needs to enforce the rule

$$f_s > 2\left(f_c + \frac{\beta}{T}\right), \quad (2)$$

where $\beta \in \mathbb{R}^+$ is a 'roll-off' parameter that depends on $g(t)$. Using square brackets to denote discretized signals, we set

$$\ell_I[n,\phi] = \ell_I(n/f_s,\phi)/\sqrt{f_s} \quad \text{and}$$
$$\ell_Q[n,\phi] = \ell_Q(n/f_s,\phi)/\sqrt{f_s},$$

where $f_s = N/T$ and $N \in \mathbb{R}^+$. This ensures the orthonormality of $\ell_I[n,\phi]$ and $\ell_Q[n,\phi]$ in the discrete domain. Therefore, on sampling $r(t)$ in (1) and *normalizing* by $\sqrt{f_s}$, we have the discretized passband equation:

$$r[n] = |h|\big(x_I\ell_I[n,\phi] + x_Q\ell_Q[n,\phi]\big) + w[n] \quad (3)$$

$\forall\ n \in \{1, 2, \ldots, N\}$. Finally, we note that the random variables corresponding to h, x and $w[n]\ \forall\ n \in \{1, 2, \ldots, N\}$ are independent of each other.

2.2 The αSGN(m) Process

The distribution of a stable *random variable* is fully characterized by four parameters and is denoted by $\mathcal{S}(\alpha, \beta, \delta, \mu)$ [18, 20, 23]. Precisely, $\alpha \in (0, 2]$ is the *characteristic exponent*, $\beta \in [-1, 1]$ is the skew parameter, $\delta \in (0, +\infty)$ is the scale and $\mu \in (-\infty, +\infty)$. Of these, α determines the heaviness of the tails in the distribution. The smaller the value of α, the heavier the tails. In fact, for $\alpha = 2$, the distribution is independent of β and is equivalent to a Gaussian distribution with mean μ and variance $2\delta^2$, i.e., $\mathcal{N}(\mu, 2\delta^2)$ [18, 20, 23]. If β and μ are equated to zero, the distribution reduces to that of a SαS random variable and is denoted by the abridged notation $\mathcal{S}(\alpha, \delta)$ [12]. As highlighted by its name, a SαS PDF is symmetric about zero and is also unimodal. Do note that $\mathcal{S}(2, \delta) \stackrel{d}{=} \mathcal{N}(0, 2\delta^2)$, where the symbol $\stackrel{d}{=}$ implies equality in distribution.

A *random vector* $\vec{W} \in \mathbb{R}^m$ is α-sub-Gaussian if it can be expressed as

$$\vec{W} \stackrel{d}{=} A^{1/2}\vec{G}, \quad (4)$$

where $\vec{G}$ is a zero-mean m-dimensional Gaussian vector with the $m \times m$ covariance matrix $\mathbf{\Sigma} = [\sigma_{ij}]$, i.e., $\vec{G} \sim \mathcal{N}(\mathbf{0}, \mathbf{\Sigma})$, and $A \sim \mathcal{S}(\frac{\alpha}{2}, 1, 2(\cos(\frac{\pi\alpha}{4}))^{2/\alpha}, 0)$ is a totally right-skewed heavy-tailed stable random variable [18, 19, 23]. Both A and $\vec{G}$ are statistically independent of each other. Due to the underlying $\vec{G}$, the PDF of $\vec{W}$ is also unimodal and depicts elliptical geometries. However, the latter will have heavy (algebraic) tails. Denoting the i^{th} element of $\vec{W}$ as W_i, we have $W_i \sim \mathcal{S}(\alpha, \sqrt{\sigma_{ii}})$ [19]. In some texts, the multiplicative factor of 2 is omitted from the scale parameter of A, which results in $W_i \sim \mathcal{S}(\alpha, \sqrt{\sigma_{ii}/2})$ [18, 23]. We stick to the former definition.

The αSGN(m) model is based on a sliding-window framework and enforces any immediately adjacent $m+1$ samples to be α-sub-Gaussian [13]. The $(m+1) \times (m+1)$ covariance matrix of the underlying Gaussian vector corresponding to these samples is denoted by $\mathbf{C}_m = [c_{ij}]$. The process is stationary and therefore $\mathbf{C}_m$ does not vary with time. Due to the sliding-window, the process is Markovian with order m. Specifically, if $\vec{W}_{n,m} = [W_{n-m}, W_{n-m+1}, \ldots, W_n]^\mathsf{T}$ is a random vector consisting of the current sample (at index n)

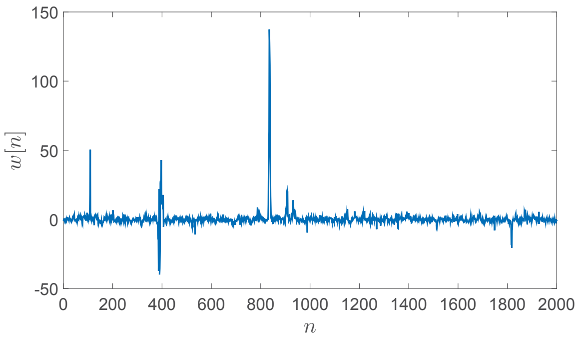

Figure 1: A realization of αSGN(1) with $\mathbf{C}_1$ in (7) and $\alpha = 1.5$.

and m immediately previous samples of an αSGN(m) process, then from (4) we have

$$\vec{W}_{n,m} \overset{d}{=} A_n^{1/2} \vec{G}_{n,m} \tag{5}$$

$\forall\ n \in \mathbb{Z}$, where $\vec{G}_{n,m} = [G_{n-m}, G_{n-m+1}, \ldots, G_n]^\intercal$ is a Gaussian random vector with distribution $\mathcal{N}(\mathbf{0}, \mathbf{C}_m)\ \forall\ n \in \mathbb{Z}$. Due to the sliding-window framework, it is not hard to ascertain that $\mathbf{C}_m$ is a *symmetric Toeplitz matrix* [13]. Hence, $r_{ii} = r_{jj}\ \forall\ i,j \in \{1, 2, \ldots, m+1\}$ and therefore

$$W_i \overset{d}{=} W_j \sim \mathcal{S}(\alpha, \delta_w) \tag{6}$$

$\forall\ i,j \in \mathbb{Z}$, where $\delta_w = \sqrt{r_{ii}}$. We also note that the underlying $G_n\ \forall\ n \in \mathbb{Z}$ is essentially a Gaussian autoregressive process of order m (AR(m)).

As an example, we present a realization of an αSGN(1) process (denoted by $w[n]$) in Fig. 1 and show its delay scatter plots in Fig. 2 for delays of 1, 2, 5 and 40. We consider $\alpha = 1.5$ and

$$\mathbf{C}_1 = \begin{bmatrix} 1 & 0.7 \\ 0.7 & 1 \end{bmatrix}. \tag{7}$$

One can clearly see the bursts within the realization and the elliptic geometry on the scatter plot with unit delay. When the delay is large enough, we get a four-tailed scatter plot, which implies near-independence of samples [12]. For the special case of $m = 0$, the αSGN(m) reduces to the WSαSN process. The scatter plots in this instance will correspond to a four-tailed configuration for all delays [12]. For more details about αSGN(m), refer to [13].

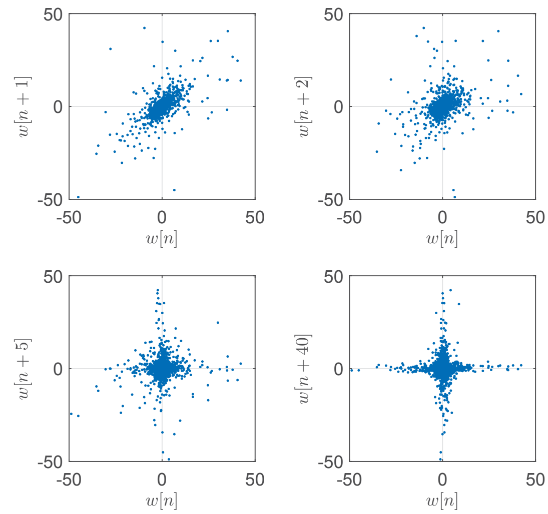

Figure 2: Delay scatter plots of an αSGN(1) process with $\mathbf{C}_1$ in (7) and $\alpha = 1.5$.

3. CONVENTIONAL ROBUST DETECTORS

Let $\mathbb{M}$ be the set of all possible constellation points in the complex plane. If $w[n]$ is a white noise process, then for the model in (3), the ML detector is given by

$$\hat{x} = \underset{\zeta \in \mathbb{M}}{\texttt{arg\,min}} \sum_{n=1}^{N} -\log f_W(r[n] - |h|(\mu_I \ell_I[n] - \mu_Q \ell_Q[n])), \tag{8}$$

where $\zeta = \zeta_I + j\zeta_Q$ and $f_W(\cdot)$ is the probability density function (PDF) of any sample in $w[n]$. We term (8) as the *white* ML detector (wMLD) and note that it requires complete knowledge of the noise distribution [9]. In the case of WSαSN, $f_W(\cdot)$ is a univariate SαS PDF. Depending on the scenario, one may or may not have full knowledge of the noise statistics. Further still, the wMLD may not be desirable due to the general unavailability of closed-form SαS PDFs [18, 20, 23]. One would therefore need to revert to numerical methods to evaluate the cost in (8).

From generalized ML theory [8], one may express (8) as

$$\hat{x} = \underset{\zeta \in \mathbb{M}}{\texttt{arg\,min}} \sum_{n=1}^{N} -\log \rho(r[n] - |h|(\mu_I \ell_I[n] - \mu_Q \ell_Q[n])), \tag{9}$$

where $\rho(\cdot) \in \mathbb{R}^+$. Ideally, $\rho(\cdot)$ should be as similar to $f_W(\cdot)$ as possible [16]. In the literature, various expressions for $\rho(\cdot)$ have been employed to achieve this [1,2]. We will focus on two such functions:

1. The L_p-norm detector (L_pD), for $p < 2$ [2,16]:
$$\log \rho(x) = -|x|^p \tag{10}$$

2. The geometric mean detector (GMD) [5,12]:
$$\log \rho(x) = -\log |x| \tag{11}$$

Both the above functions have *closed-forms* and are *symmetric* in x. Moreover, the L_pD and GMD do not require any prior knowledge of the parameters of the noise process and are therefore *non-parametric*.

The detectors highlighted in this section are known to be robust in white impulsive noise. However, they do not take the dependence between noise samples into account. This is fine if the noise process is WSαSN, but it is yet to be established how they perform in comparison to the optimal (ML) detector in αSGN(m). The latter is derived next.

4. ROBUST DETECTORS IN αSGN(m)

Let $\vec{W}_N = [W_1, W_1, \ldots, W_N]^\intercal$ be a random vector of N samples of a noise process. We denote the joint-PDF of $\vec{W}$ by $f_{\vec{W}_N}(\mathbf{w}_N)$, where $\mathbf{w}_N = [w_1, w_2, \ldots, w_N]^\intercal$ is a sample outcome. We can express it as a product of *univariate* conditional densities [21], i.e.,

$$f_{\vec{W}_N}(\mathbf{w}_N) = f_{\vec{W}_m}(\mathbf{w}_m) \prod_{n=m+1}^{N} f_{W_n|\vec{W}_{n-1}}(w_n|\mathbf{w}_{n-1}),$$

which leads to

$$f_{\vec{W}_N}(\mathbf{w}_N) = \prod_{n=1}^{m} f_{W_n|\vec{W}_{n-1}}(w_n|\mathbf{w}_{n-1}) \times \prod_{n=m+1}^{N} f_{W_n|\vec{W}_{n-1}}(w_n|\mathbf{w}_{n-1}). \quad (12)$$

If W_n is an αSGN(m) process, then as it is Markov of order m, (12) simplifies to

$$f_{\vec{W}_N}(\mathbf{w}_N) = \prod_{n=1}^{m} f_{W_n|\vec{W}_{n-1}}(w_n|\mathbf{w}_{n-1}) \times \prod_{n=m+1}^{N} f_{W_n|\vec{W}_{n-1,m-1}}(w_n|\mathbf{w}_{n-1,m-1}), \quad (13)$$

where $\mathbf{w}_{n,m} = [w_{n-m}, w_{n-m+1}, \dots, w_n]^\mathsf{T}$ is a vector of $m+1$ immediately adjacent αSGN(m) samples at index n. Finally, as the process is stationary, we get

$$f_{\vec{W}_N}(\mathbf{w}_N) = \prod_{n=1}^{m} f_{W_n|\vec{W}_{n-1}}(w_n|\mathbf{w}_{n-1}) \times \prod_{n=m+1}^{N} f_{W_{m+1}|\vec{W}_m}(w_n|\mathbf{w}_{n-1,m-1}). \quad (14)$$

Letting $w_n = w[n]$, the αSGN(m) ML detector of x is

$$\hat{x} = \underset{\zeta\in\mathbb{M}}{\mathtt{arg\,min}} - \Big(\sum_{n=1}^{m} f_{W_n|\vec{W}_{n-1}}(w_n|\mathbf{w}_{n-1}) + \sum_{n=m+1}^{N} \log f_{W_{m+1}|\vec{W}_m}(w_n|\mathbf{w}_{n-1,m-1}) \Big), \quad (15)$$

where from (3) we have

$$w_n = r[n] - |h|\big(\zeta_I \ell_I[n,\phi] + \zeta_Q \ell_Q[n,\phi]\big). \quad (16)$$

As mentioned in Section 2.2, the αSGN(m) model is based on a Gaussian AR(m) process. Such processes have been studied extensively in the literature [7,21]. Due to its structure, one may write $\mathbf{C}_m$ in the block matrix form

$$\mathbf{C}_m = \begin{bmatrix} \mathbf{C}_{m-1} & \mathbf{c}_m \\ \mathbf{c}_m^\mathsf{T} & c_{(m+1)(m+1)} \end{bmatrix}, \quad (17)$$

where $\mathbf{r}_m = [r_{1(m+1)}, r_{2(m+1)}, \dots, r_{m(m+1)}]^\mathsf{T}$. Using the above expression, one can mathematically express the AR(m) process as

$$G_n = \mathbf{r}_m^\mathsf{T} \mathbf{C}_{m-1}^{-1} \mathbf{g}_{n-1,m-1} + \sqrt{\frac{\det \mathbf{C}_m}{\det \mathbf{C}_{m-1}}} Z_n, \quad (18)$$

where $\vec{G}_{n-1,m-1} = \mathbf{g}_{n-1,m-1}$ and $Z_n \sim \mathcal{N}(0,1)$ are IID $\forall\, n \in \mathbb{Z}$ [14]. As G_n is a stationary process,

$$G_n|\vec{G}_{n-1,m-1} \overset{d}{=} G_{m+1}|\vec{G}_m.$$

From (18), one can clearly see that $G_{m+1}|\vec{G}_m = \mathbf{g}_{n-1,m-1}$ is Gaussian with *mean* $\mathbf{r}_m^\mathsf{T}\mathbf{C}_{m-1}^{-1}\mathbf{g}_{n-1,m-1}$. In fact, one may extend these observations to the univariate conditional PDFs of the αSGN(m) process found in the latter product term of (14). Precisely, the PDF of $W_{m+1}|\vec{W}_m = \mathbf{w}_{n-1,m-1}$ is a *unimodal shifted symmetric* distribution, with *location* given by

$$\mu_{m,n} = \mathbf{r}_m^\mathsf{T}\mathbf{C}_{m-1}^{-1}\mathbf{w}_{n-1,m-1}.$$

However, unlike their Gaussian counterparts the PDF is heavy-tailed. The actual derivations of these properties are somewhat involved [14] and are beyond the scope of this text. Using a similar argument for the prior product term in (14), the PDF of $W_n|\vec{W}_{n-1} = \mathbf{w}_{n-1}\ \forall\, n \in \{1,2,\dots,m\}$ is also a *unimodal shifted symmetric* distribution, with *location*

$$\mu_n = \mathbf{r}_{n-1}^\mathsf{T}\mathbf{C}_{n-2}^{-1}\mathbf{w}_{n-1}.$$

If one were to extend the generalized ML framework [8] to αSGN(m) processes, we first note that

$$f_{W_n|\vec{W}_{n-1}}(w_n|\mathbf{w}_{n-1}) = f_{W_n-\mu_n|\vec{W}_{n-1}}(w_n-\mu_n|\mathbf{w}_{n-1}),$$

$\forall\, n \in \{1,2,\dots,m\}$ and

$$f_{W_{m+1}|\vec{W}_m}(w_n|\mathbf{w}_{n-1,m-1}) = f_{W_{(m+1)}-\mu_{m,n}|\vec{W}_m}(w_n-\mu_{m,n}|\mathbf{w}_{n-1,m-1}),$$

where the latter terms in both equations correspond to symmetric PDFs. Therefore, analogous to (9), we can modify (15) to

$$\hat{x} = \underset{\zeta\in\mathbb{M}}{\mathtt{arg\,min}} - \Big(\sum_{n=1}^{m} \log\rho(w_n-\mu_n) + \sum_{n=m+1}^{N} \log\rho(w_n-\mu_{m,n}) \Big) \quad (19)$$

where w_n is given by (16) and $\rho(\cdot) \in \mathbb{R}^+$ is a *symmetric* function. One may use the functions in (10) and (11) to get the location-corrected L_pD (lc-L_pD)

$$\hat{x} = \underset{\zeta\in\mathbb{M}}{\mathtt{arg\,min}} \sum_{n=1}^{m} |w_n-\mu_n|^p + \sum_{n=m+1}^{N} |w_n-\mu_{m,n}|^p$$

and the location-corrected GMD (lc-GMD) detector

$$\hat{x} = \underset{\zeta\in\mathbb{M}}{\mathtt{arg\,min}} \sum_{n=1}^{m} \log|w_n-\mu_n| + \sum_{n=m+1}^{N} \log|w_n-\mu_{m,n}|,$$

respectively. We note that both aforementioned schemes are now *parametric*. However, the only information they require is that of $\mathbf{C}_m$ and no knowledge of α is necessary. As $\mathbf{C}_m$ is a symmetric Toeplitz matrix, only one row (or column) is required for its construction.

5. RESULTS & DISCUSSION

5.1 SNR Definition

Before we present our results, it is necessary that we define a signal-to-noise ratio (SNR) measure. We can use approaches similar to those employed in [12, 16, 18]. In the additive white Gaussian noise (AWGN) case, error performance is plotted against the average SNR per bit [22], i.e., $\mathcal{E}_b/N_0$, where $\mathcal{E}_b$ is the received signal energy per bit averaged over h and the employed constellation, and $N_0/2$ is the two-sided power spectral density (PSD) of the white noise process. One can evaluate the average received signal energy, $\mathcal{E}_s = \mathcal{E}_b \log_2 M$, from either (1) or (3):

$$\begin{aligned}\mathcal{E}_s &= E_h[|h|^2] \int_0^T E_x[\big(x_I \ell_I(t,\phi) + x_Q \ell_Q(t,\phi)\big)^2]\mathrm{d}t \\ &= E_h[|h|^2] \sum_{n=1}^{N} E_x[\big(x_I \ell_I[n,\phi] + x_Q \ell_Q[n,\phi]\big)^2] \\ &= E_h[|h|^2] E_x[|x|^2] = \sigma_h^2 \mathcal{E}_x,\end{aligned}$$

where $E_h[\cdot]$ and $E_x[\cdot]$ are the expectation operators with respect to h and x, respectively, and $E_x[|x|^2] = \mathcal{E}_x$. As stated in [12, 18], N_0 has no physical interpretation for a stable process as the second order moments of stable random variables do not converge. From (1) and (3), we see that $w[n]\ \forall\ n \in \mathbb{Z}$ are IID outcomes from $\mathcal{N}(0, N_0/2)$ if $w(t)$ is an AWGN process [22]. From the discussion in Section 2.2, we have $\mathcal{N}(0, 2\delta_w^2) \stackrel{d}{=} \mathcal{S}(2, \delta_w)$, where δ_w is the scale of $W_n\ \forall\ n \in \{1, 2, \ldots, N\}$. We can therefore express N_0 in terms of the scale of a SαS random variable, i.e., $N_0 = 4\delta_w^2$ [12]. The resulting SNR measure is then

$$\frac{\mathcal{E}_b}{N_0} = \frac{\sigma_h^2 \mathcal{E}_x}{4\delta_w^2 \log_2 M}. \tag{20}$$

Do note that for an αSGN(m) process, we have from (6), $\delta_w = \sqrt{r}_{ii}\ \forall\ i \in \{1, 2, \ldots, m+1\}$.

5.2 Results

For our simulations, we consider an αSGN(4) process with the *normalized* covariance matrix $\acute{\mathbf{C}}_4 = \mathbf{C}_4/\delta_w^2$ given by

$$\acute{\mathbf{C}}_4 = \begin{bmatrix} 1.0000 & 0.5804 & 0.2140 & 0.1444 & -0.0135 \\ 0.5804 & 1.0000 & 0.5804 & 0.2140 & 0.1444 \\ 0.2140 & 0.5804 & 1.0000 & 0.5804 & 0.2140 \\ 0.1444 & 0.2140 & 0.5804 & 1.0000 & 0.5804 \\ -0.0135 & 0.1444 & 0.2140 & 0.5804 & 1.0000 \end{bmatrix}. \tag{21}$$

Using the method outlined in [13], $\acute{\mathbf{C}}_4$ was estimated from empirical noise data observed in the warm shallow underwater channel at a sampling rate of 180 kHz. The dataset was recorded in Singapore waters by staff of the Acoustic Research Laboratory (ARL) at the National University of Singapore. We analyze the error performance of the wMLD, L_1D and GMD presented in Section 3 and the MLD, lc-L_1D and lc-GMD in Section 4. Results are compiled for the severely ($\alpha = 1.5$) and slightly ($\alpha = 1.9$) impulsive noise cases and the receiver is expected to have complete knowledge of the channel. We use $N = 10$ for our simulations as it may not be possible to set $N = f_s T$ to a large value in practice. Nevertheless, we do analyze the effect of N on the performance as well.

In Fig. 3, we plot the bit error rate (BER) curves of a binary phase shift keying (BPSK) system for $\alpha = 1.5$. Surprisingly, the L_1D performs better than the wMLD. This may be due to the fact that the latter over emphasizes the whiteness assumption due to complete knowledge of α and

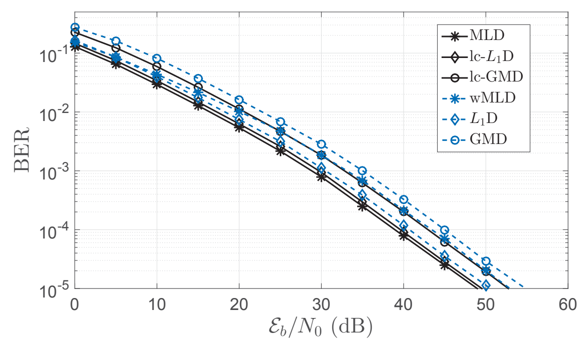

Figure 3: BPSK BER performance in αSGN(4) for $\alpha = 1.5$, $N = 10$ and $\acute{\mathbf{C}}_4$ in (21).

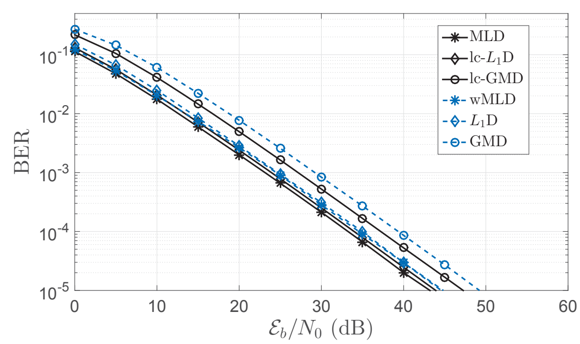

Figure 4: BPSK BER performance in αSGN(4) for $\alpha = 1.9$, $N = 10$ and $\acute{\mathbf{C}}_4$ in (21).

δ_w. The BER performance of the lc-L_1D is close to that of the optimal detector. Between the ML detectors, there is a gain of $\sim$ 5dB. As expected, one also sees improvements between the lc-L_1D and lc-GMD with respect to their conventional counterparts. For the former there is a $\sim$ 1dB improvement, while for the latter there is a $\sim$ 2dB improvement for a large range of SNR. On the whole, the L_1D is a good choice if the receiver has no information about the impulsive noise process.

For $\alpha = 1.9$, we present the BPSK BER performance in Fig. 4. One sees similar trends as those in Fig. 3, but as expected, the results are better over all as the noise is less impulsive. The L_1D's performance is slightly worse than that of the wMLD and is $\sim$ 0.8dB worse than the lc-L_1D. The lc-GMD is still $\sim$ 2dB better than the GMD. Moreover, the MLD offers a $\sim$ 0.8dB gain over the wMLD.

In [12,16], the authors consider the WSαSN model with no fading and show that there is significant improvement in the BER detection performance of a single-carrier system when N is increased. This is due to the fact that the information of a noise impulse is spread over a bandwidth much larger than that of the signal. On employing suitable detectors, higher values of N allow the receiver to harness the information within this extended bandwidth. When the channel depicts Rayleigh block fading, the BER improvement still exists, but is notably smaller [12, 15]. In Fig. 5, we show how the BER performance of the optimal detector in αSGN(m) for the $\alpha = 1.5$ case changes with N. At large SNR, the gain

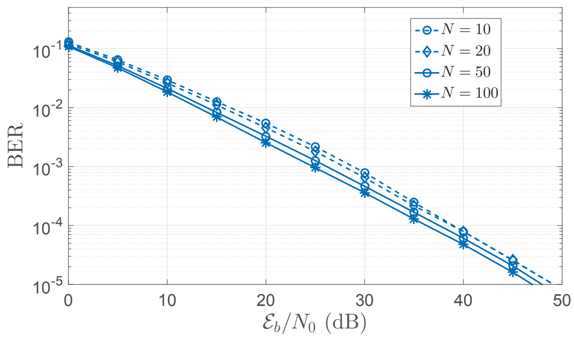

Figure 5: BPSK BER performance of the MLD for various N. The αSGN(4) model with $\alpha = 1.5$ and $\acute{\mathbf{C}}_4$ in (21) is employed.

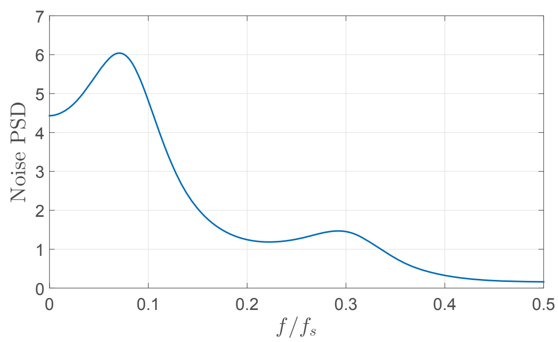

Figure 6: PSD of the Gaussian AR(4) process corresponding to $\acute{\mathbf{C}}_4$ in (21).

of the $N = 100$ case over $N = 10$ is $\sim$ 2dB. From ML estimation theory, we know that soft-estimates of $\hat{x}$ tend to a Gaussian distribution as $N \to \infty$ [9]. This why the curve for $N = 100$ 'straightens' out and is akin to what one finds in block Rayleigh fading channels with AWGN [22, 26]. On the other hand, for $\alpha = 1.9$, one can see the BER curve corresponding to the optimal detector already flattened out for $N = 10$ in Fig. 4. There is no noticeable improvement in performance on increasing N any further (not shown here).

5.3 Carrier Placement

Due to the dependence between samples of $w[n]$, one would expect its spectrum not to be flat. As stated in Section 5.1, the PSD of a stable process does not converge as second order moments of stable random variables are infinite [18]. However, for an αSGN(m) process, one may define the PSD of the underlying Gaussian AR(m) process as its *pseudo*-PSD [16]. The latter signifies the spectral shape of the αSGN(m) process. In Fig. 6, we present the one-sided PSD of the Gaussian AR(m) process for $\acute{\mathbf{C}}_m$ in (21) with $\delta_w = 1$. Here f/f_s is the normalized frequency. Note that the pseudo-PSD will be the same *irrespective* of what α may be.

Detection in colored Gaussian noise is a well-studied area [26, 27]. A typical routine is to place the carrier (and thus the passband signal) in a low PSD noise regime. This approach is optimal for wide sense stationary (WSS) noise with large data records [9]. For the simulations carried out in Sec-

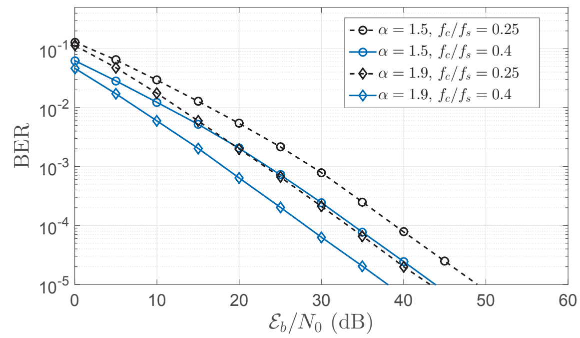

Figure 7: Effect of carrier placement in αSGN(4) with $\acute{\mathbf{C}}_4$ in (21) for $N = 10$.

tion 5.2, $f_c/f_s = 0.25$. As the constraint in (2) needs to be adhered to, we plot the BER for the MLD with $f_c/f_s = 0.4$ in Fig. 7. As before, the curves are generated for BPSK with $N = 10$. For comparison, we also re-plot the BER for the MLD achieved with $f_c/f_s = 0.25$ and $N = 10$. The SNR gain due to good carrier placement is in excess of 5dB for both the $\alpha = 1.5$ and $\alpha = 1.9$ cases. Therefore, by using smart carrier placement in conjunction with a suitable robust detector, the BER performance of a single-carrier system can be improved.

6. CONCLUSION

We proposed and analyzed various detectors for a single-carrier communication scheme operating in αSGN(m) with Rayleigh block fading. The αSGN(m) model was specifically developed in the literature to model the ambient noise observed in warm shallow waters. In our work, the ML detector was derived and generalized ML estimation theory was extended to cover the αSGN(m) framework. The resulting robust detectors were shown to harness the dependence between the noise samples and outperformed their conventional parts. Taking BPSK as an example case, BER analysis was conducted for both severely and slightly impulsive noise channels. Variations against the number of samples per transmitted symbol and carrier placement were investigated and commented on. For future work, a more rigorous treatment to signal placement may be conducted. The baseband model needs to be developed, and with it, baseband schemes may be designed.

7. REFERENCES

[1] G. Arce. *Nonlinear signal processing: a statistical approach*. Wiley InterScience online books. Wiley-Interscience, 2005.

[2] M. Chitre, J. Potter, and S. Ong. Viterbi decoding of convolutional codes in symmetric α-stable noise. *IEEE Communication Letters*, 55(12):2230 –2233, Dec. 2007.

[3] M. Chitre, J. Potter, and S.-H. Ong. Optimal and near-optimal signal detection in snapping shrimp dominated ambient noise. *IEEE Journal of Oceanic Engineering*, 31(2):497 –503, April 2006.

[4] D. Fertonani and G. Colavolpe. On reliable communications over channels impaired by bursty impulse noise. *IEEE Transactions on Communications*, 57(7):2024–2030, July 2009.

[5] J. Gonzalez, J. Paredes, and G. Arce. Zero-order statistics: A mathematical framework for the processing and characterization of very impulsive signals. *IEEE Transactions on Signal Processing*, 54(10):3839 –3851, Oct. 2006.

[6] J. G. Gonzalez and G. R. Arce. Statistically-efficient filtering in impulsive environments: weighted myriad filters. *EURASIP Journal on Advances in Signal Processing*, 2002:4–20, January 2002.

[7] J. Hamilton. *Time Series Analysis*. Princeton University Press, 1994.

[8] P. Huber and E. Ronchetti. *Robust Statistics*. Wiley Series in Probability and Statistics. John Wiley & Sons, Inc., 2009.

[9] S. Kay. *Fundamentals of Statistical Signal Processing: Detection theory*. Prentice Hall Signal Processing Series. Prentice-Hall PTR, 1998.

[10] M. Legg, A. Zaknich, A. Duncan, and M. Greening. Analysis of impulsive biological noise due to snapping shrimp as a point process in time. In *OCEANS 2007 - Europe*, pages 1–6, 2007.

[11] M. W. Legg. *Non-Gaussian and non-homogeneous Poisson models of snapping shrimp noise*. PhD thesis, Curtin Univ. of Technology, 2009.

[12] A. Mahmood. *Digital Communications in Additive White Symmetric Alpha-Stable Noise*. PhD thesis, Natl. Univ. of Singapore, June 2014.

[13] A. Mahmood and M. Chitre. Modeling colored impulsive noise by markov chains and alpha-stable processes. In *Oceans - Genoa, 2015*, pages 1–7, May 2015.

[14] A. Mahmood and M. Chitre. Generating random variates for stable sub-Gaussian processes with memory. *Signal Processing*, to be published.

[15] A. Mahmood, M. Chitre, and M. A. Armand. Detecting OFDM signals in alpha-stable noise. *IEEE Transactions on Communications*, 62(10):3571–3583, Oct 2014.

[16] A. Mahmood, M. Chitre, and M. A. Armand. On single-carrier communication in additive white symmetric alpha-stable noise. *IEEE Transactions on Communications*, 62(10):3584–3599, Oct 2014.

[17] G. Ndo, F. Labeau, and M. Kassouf. A Markov-Middleton model for bursty impulsive noise: Modeling and receiver design. *IEEE Transactions on Power Delivery*, 28(4):2317–2325, oct 2013.

[18] C. L. Nikias and M. Shao. *Signal processing with Alpha-Stable Distributions and Applications*. Chapman-Hall, New York, 1996.

[19] J. P. Nolan. Multivariate elliptically contoured stable distributions: theory and estimation. *Computational Statistics*, 28(5):2067–2089, 2013.

[20] J. P. Nolan. *Stable Distributions - Models for Heavy Tailed Data*. Birkhauser, Boston, 2015. In progress, Chapter 1 online at.

[21] A. Papoulis and U. S. Pillai. *Probability, Random Variables and Stochastic Processes*. McGraw-Hill, Boston, Dec 2001.

[22] J. Proakis and M. Salehi. *Digital Communications*. McGraw-Hill higher education. McGraw-Hill Education, 2007.

[23] G. Samorodnitsky and M. S. Taqqu. *Stable Non-Gaussian Random Processes: Stochastic Models with Infinite Variance*. Chapman & Hall, 1994.

[24] T. Shongwey, A. Vinck, and H. Ferreira. On impulse noise and its models. In *18th IEEE International Symposium on Power Line Communications and its Applications (ISPLC)*, pages 12–17, March 2014.

[25] M. Stojanovic and J. Preisig. Underwater acoustic communication channels: Propagation models and statistical characterization. *IEEE Communications Magazine*, 47(1):84–89, January 2009.

[26] D. Tse and P. Viswanath. *Fundamentals of Wireless Communication*. Wiley series in telecommunications. Cambridge University Press, 2005.

[27] C. Weber. *Elements of Detection and Signal Design*. Springer Texts in Electrical Engineering. Springer New York, 2012.

[28] M. Zimmermann and K. Dostert. Analysis and modeling of impulsive noise in broad-band powerline communications. *IEEE Transactions on Electromagnetic Compatibility*, 44(1):249 –258, Feb 2002.